International Journal of GEOMATE, March., 2024 Vol.26, Issue 115, pp.73-80
ISSN: 2186-2982 (P), 2186-2990 (O), Japan, DOI: https://doi.org/10.21660/2024.115.g13171
Geotechnique, Construction Materials and Environment

THE PHYSICAL AND MECHANICAL PROPERTIES OF SINGLE PUMICE SAND PARTICLE

* I Wayan Ariyana Basoka[1,4], *Kiyonobu Kasama[1], Zentaro Furukawa[2], Noriyuki Yasufuku[1], Ahmad Rifa'i[3]

[1]Department of Civil Engineering, Kyushu University, Fukuoka, Japan;
[2]Faculty of Environmental and Life Science, Okayama University, Okayama, Japan;
[3]Department of Civil and Environmental Engineering, Universitas Gadjah Mada, Yogyakarta, Indonesia;
[4]Departement of Civil Engineering, Universitas Warmadewa, Bali, Indonesia.

*Corresponding Author, Received: 06 Sep. 2023, Revised: 9 Jan. 2024, Accepted: 10 Jan. 2024

ABSTRACT: Pumice sand is a volcanic material widely distributed in volcanic areas such as Japan, Indonesia, and countries traversed by volcanic mountains. Geotechnical problems regarding pumice sand often occur in these areas, such as landslides because of the pumice crushable structure. Based on previous research, some failure phenomena are caused by the existing pumice layer, and not so many studies describe the behavior of pumice single particle located at Kyushu Island, Japan. This study conducted a series of tests to clarify pumice material's microscopic and mechanical properties. Scanning Electron Microscopy (SEM) and Energy Dispersive Spectroscopy (EDS) tests were carried out on pumice materials to determine the microscopic and chemical compounds in the pumice material. Then, single-particle crushability tests were carried out as representative of the mechanical behavior of pumice sand particles. The approach using linear regression fitting is carried out using conventional frequentist and Bayesian hierarchical approaches to obtain the strength behavior of the pumice sand. An overview of pumice microscopy conditions and minerals can be helpful when ground improvement and soil stabilization are discussed for this pumice material and the effect of particle shape on pumice strength is observed. According to this study, oxygen, silica, and alumina dominate pumice sand chemical components. The aspect ratio and the roundness coefficient of pumice sand do not significantly impact particle stress. Particle size reduces and increases particle stress in single-particle crushability tests. Single-particle crushability reduces pumice particle pore area and increases the number of pores.

Keywords: Pumice, Scanning electron microscopy, Single-particle strength, Particle shape

1. INTRODUCTION

Pyroclastic rocks comprise discrete particles that are ejected from volcanic vents as a result of explosions. A variety of pyroclastic deposits are generated by explosive volcanic eruptions [1, 2]. The pyroclastic fragments, such as pumice and glass fragments, exhibit distinct characteristics. The rapid formation of pyroclastic fragments is a characteristic feature, which is a clear contrast to the gradual disintegration of general rocks caused by the processes of weathering and erosion. Pumice, a glassy volcanic rock with high pores, is white or pale grey to brown in color; pumice sand is subject to pulverization during seismic events, which may potentially induce landslides and liquefaction. Several regions with active volcanoes, including Indonesia, Japan, New Zealand, and the United States, exhibit pumice layers in multiple locations at some points attributed to the failure, which causes landslides or liquefaction phenomena [3–7]. To fully understand the behavior of pumice particles, it is crucial to consider both the general properties of pumice and the failures resulting from the presence of the pumice layer. A group of researchers performed individual particle strength tests to characterize the behavior of the particles in a material [8–13]. The primary objective of the single-particle test is to assess the capacity of individual particles to endure compression or fracture when subjected to a specific force and to ascertain the mechanical strength of the particles being examined [14, 15].

Previous studies were conducted by Orense R. P., Pender M. J., Hyodo M., and Nakata Y. [16]. Regarding the characteristics of pumice using pumice material originating from New Zealand, several tests were carried out to describe the characteristics of this pumice, such as single particle test, SEM, and monotonic and cyclic triaxial tests. The results of single-particle strength show that the strength is lower than silica sand grains. Then Kasama K., Furukawa Z., and Yasufuku N. [5] also researched pumice, for which pumice material was obtained from Takanodai Village, Minami Aso, Kumamoto, Kyushu, Japan. In this place, a landslide had occurred on a relatively gentle slope. In the initial investigation, it was suspected that a pumice layer had become the slip surface potential. Several tests were carried out on this study, such as single particle strength, cyclic box shear test, and numerical modeling. Based on that study, it is known that pumice has a character that is easily crushed, where the single-particle strength value is also lower than silica sand materials in general. Sumartini W. O., Hazarika H., Kokusho T., Ishibashi S., Matsumoto D., and Chaudhary B. [17] also conducted a study at the same location at Takanodai Village by carrying out SEM, chemical component, and triaxial cyclic tests. In this study, the effect of liquefaction of pumice material on earthquakes was observed. Furthermore, there was also research conducted by Kikkawa N., Pender M. J., and Orense R. P. [18], which compared the geotechnical properties of pumice sand from the Osumi-peninsula in Southern Kyushu, Japan, and New Zealand. The tests carried out were the drain triaxial test and sieve analysis. These studies showed that the properties of the materials were very similar despite their different origins and particle size distributions.

Based on an explanation of pumice studies by previous researchers, most of the approach used was conventional frequentist. The uncertainties are not quickly addressed under the frequentist thinking framework but rather necessitate Bayesian reasoning. Bayesian thinking pertains to the processes of judgment and belief. This phenomenon results in highly significant deductions even when the available data is limited [19, 20]. Whereas in this research, the approach used Bayesian methods that can handle complex models and hierarchical structures more efficiently than frequentist methods, and there are limited studies on the single-particle strength of pumice in various locations, particularly in the Kyushu area. Based on some failure phenomena caused by pumice material, it is crucial to understand the properties of individual pumice sand, especially pumice particles, to illustrate the microstructural behavior of pumice as a basis for the following study.

This study aims to discover particle pumice characteristics by carrying out SEM, EDS, and single-particle strength behavior using Bayesian approach, which previous researchers have not mentioned. Furthermore, discovering the influence of particle shape on single-particle strength is also conducted in this study. This study consists of 7 parts: introduction, research significance, material and method, results and discussion, and finally the conclusion.

2. RESEARCH SIGNIFICANCE

This research attempts to provide a comprehensive analysis of the particle properties of pumice, with a specific emphasis on the Kyushu region of Japan as the primary area of investigation. Pumice, in particular, is the subject of this investigation and has often been the cause of failure on several occasions. This study aims to improve comprehension of crushable materials in terms of microscopy and mechanical behavior. Furthermore, the analysis presented in this study provides essential insights that can be utilized to investigate crushable materials utilized in construction projects throughout future research.

3. MATERIAL AND METHOD

3.1 Material

The pumice material utilized in this study was collected at the Miyakonojo City area of Kyushu Island, Japan; this pumice is often used for agricultural purposes and sold by local companies in that area. The sample was sieved, providing the results in Fig. 1.

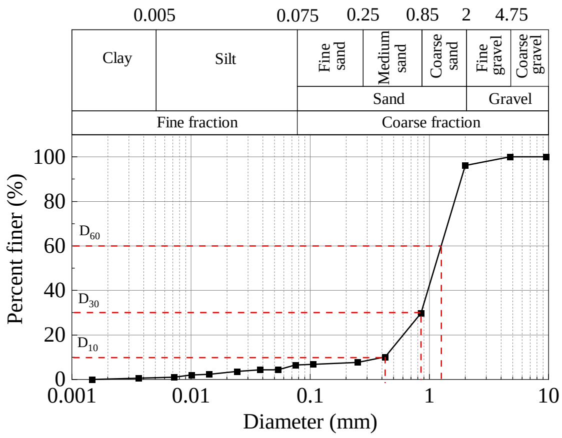

Fig. 1 Grain size distribution

The uniformity coefficient (U_u) of this sample is calculated by Eq. (1), and the coefficient of curvature (U_c') is calculated by Eq. (2).

$$U_u = \frac{D_{60}}{D_{10}} \tag{1}$$

$$U_c' = \frac{(D_{30})^2}{(D_{60} \times D_{10})} \tag{2}$$

D_{60} is the diameter of 60% passing material, D_{30} is the diameter of 30% passing material, and D_{10} is the diameter of 10% passing material. Based on this calculation, we obtained the U_u value of 2.93, which was classified as poorly graded (P) where U_u < 10, and U_c' value of 1.33. Based on the JGS 0051-2009 standard, the results can be categorized as a fine fraction <5% and a gravel fraction <5% belonging to the sand poorly graded (SP) category.

The outcomes of the sieve analysis involved the identification of three primary sizes, which were the specimens retained by the 2.000 mm sieve, the 0.850 mm sieve, and the 0.425 mm sieve. Due to the presence of a minor quantity of black sand material in the sample, it is imperative to segregate the material and solely extract the pumice material to conduct tests. Subsequently, we process the pumice substance in a dry state, as shown in Fig. 2.

Fig. 2 shows three discrete classifications of materials that are intended for analysis, specifically: (a) materials that retained a size of 2.000 mm (sample L), (b) materials that have retained a size of 0.850 mm (sample M), and (c) materials that have retained a size of 0.425 mm (sample S). The current study involved extracting 135 samples from the given set of materials, where each sample was explicitly designated for a single-particle crushability test.

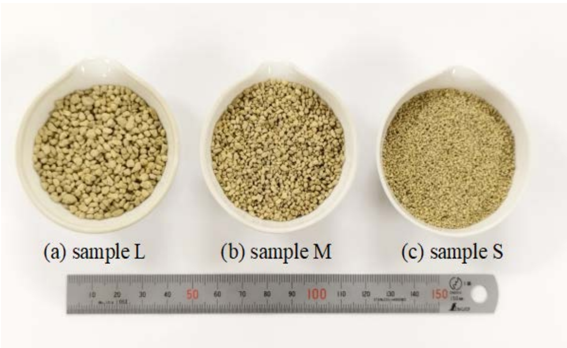

Fig. 2 Pumice sand

3.2 Microstructural and Chemical Components

The utilization of Scanning Electron Microscopy (SEM) and Energy Dispersive Spectroscopy (EDS) was conducted before and after the single-particle crushability test. Before conducting SEM and EDS testing, a platinum (Pt) coating was utilized for sample preparation. The purpose of conducting SEM testing is to visually represent the pores in pumice material before and after single-particle crushability testing. On the other hand, EDS testing aims to identify the chemical compounds present within the pumice material. In EDS analysis, it is only discussed before the crushability test because no special treatment is carried out, so it is assumed that the chemical components of the sample remain the same.

3.3 Single-Particle Crushability Test

The single-particle crushability testing was conducted by preparing the sample and performing individual testing for each particle. Initially, the dimensions of the sample were measured in terms of length, width, and height. Subsequently, a photograph of the sample was taken with a known object of reference to enable scaling and subsequent comparison with manual measurements. The testing apparatus is equipped with several components, including a load cell, sample plate, pedestal, piston, LVDT, apparatus control, data logger, and computer.

The sample was placed on a pedestal and subsequently elevated through the use of an apparatus control until the uppermost portion of the sample made contact with the load cell. The load cell utilized had a capacity of 100 N and a precision of 0.0001 N. Subsequently, an LVDT was prepared to measure the displacement of the instrument, with an LVDT precision of 0.005 mm. Once the sample, load cell, and LVDT are prepared, the instrument is adjusted to zero using a data logger application on a computer. The compression rate is set at 0.50 mm/min. Subsequently, the load cell and LVDT readings will be recorded by a data logger and transmitted to a computer.

Subsequently, the stress on the particle is calculated using Eq. (3).

$$\boldsymbol{\sigma_1 = \frac{F_1}{A}} \tag{3}$$

Where σ_1 is the first fracture stress, A is the area of the sample, F_1 is the first peak of the single-particle crushability test result as can be seen in Fig. 3. Furthermore, linear regression analysis is done using conventional methods and using the Bayesian approach in which equations for the Bayesian method can generally be seen in Eq. (4).

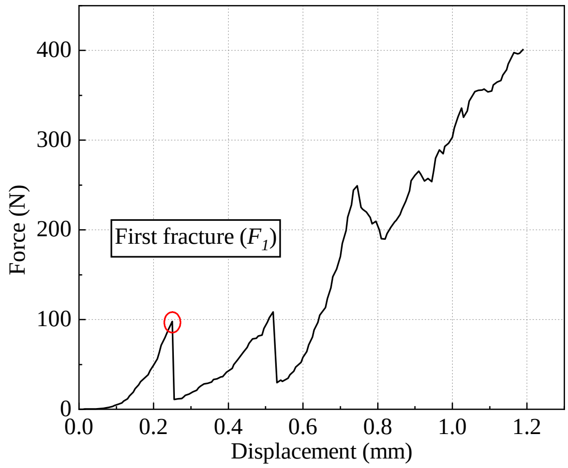

Fig. 3 Typical test result

$$\boldsymbol{p(\theta|y) = \frac{p(\theta)p(y|\theta)}{p(y)}} \tag{4}$$

The prior probability, denoted as $p(\theta)$, refers to the probability of hypothesis θ being true, irrespective of any observed evidence. The probability of the data, denoted as $p(y)$ represents the likelihood of observing the given evidence, irrespective of any specific hypothesis. The probability of data y, given that hypothesis θ is true, denoted as $p(y|\theta)$ represents the likelihood of data y

under the condition of hypothesis θ. The posterior probability, denoted as $p(\theta|y)$, represents the probability of hypothesis θ given the observed data y. In Bayesian hierarchical analysis this model uses the packages available in Python libraries.

4. RESULTS AND DISCUSSIONS

4.1 Chemical Components

The chemical component testing was conducted through EDS analysis. Before the testing, a platinum coating was applied to the pumice sample, as the high vacuum system utilized in this analysis necessitates a coating. Three sampling points were selected for EDS observation, and their average was taken. The sampling point positions can be observed in Fig. 4. Each sampling point was subsequently analyzed, and the average chemical components were obtained, as depicted in Fig. 5. Fig. 5 is an example of analysis for point spectrum 9, and the results are summarized in Fig. 6.

Fig. 6 illustrates that the most abundant chemical component is Oxygen (O) at 69.39%, Silica (Si) at 12.65%, Alumina (Al) at 7.46%, followed by other chemical components percentages below 3% for each, and total other chemical components at 10.50%. That is consistent with the findings of previous studies that reported that the chemical composition of pumice is predominantly composed of the minerals of silica (SiO_2) and alumina (Al_2O_3) [21, 22].

4.2 Particle Strength

In this study the number of tests was tried to be increased, particle strength analysis employs the conventional frequentist and Bayesian hierarchical methods to obtain a linear correlation between particle size and particle stress. Fig. 7 is the sole outcome of a Bayesian hierarchical analysis conducted after using all available data. The left figure presents the density function from the intercept and slope of the linear fitting, and the right side presents the trace from the Markov Chain Monte Carlo (MCMC) with 2000 samples.

In Fig. 8 can be seen as two statements of data fitting, with red lines presenting the frequentist method and blue lines presenting the Bayesian hierarchical method. In Fig. 8, dashed red lines from frequentist analysis can be seen in the particle stress testing indicating a negative correlation between particle size and stress, whereby an increase in sample size results in a decrease in the stress that can be sustained. The dashed-dotted red line represents the fitting based on the entire dataset, while the dashed-dotted blue line represents the fitting based on the all sample groups (sample L, M, and S) of the Bayesian hierarchical method.

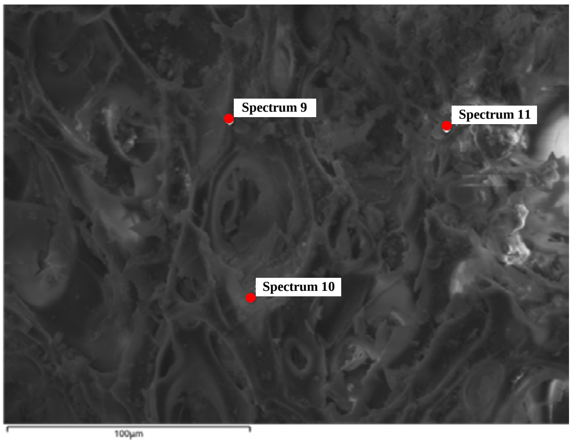

Fig. 4 EDS point sampling

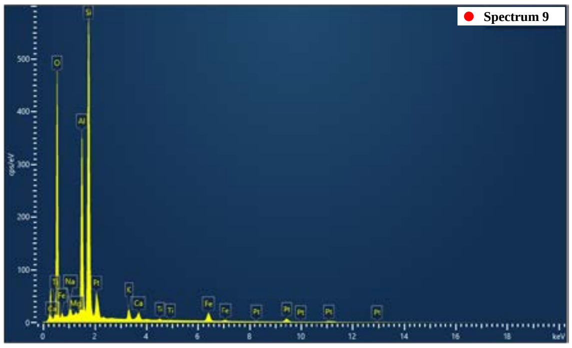

Fig. 5 EDS results

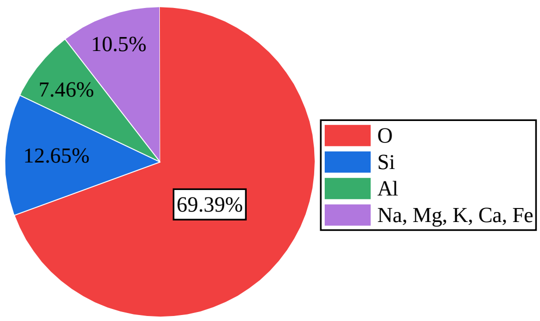

Fig. 6 Chemical component

It can be seen from the results of the Bayesian analysis in Fig. 8 that they are in line with frequentist results because due to the large volume of data used in frequentist analysis, which leads to a slight bias in interpreting the results. The linear fitting results, like those shown in Table 1, can be used as a benchmark for the relationship between particle size and particle stress in pumice particles with boundary conditions of particle size based on this study.

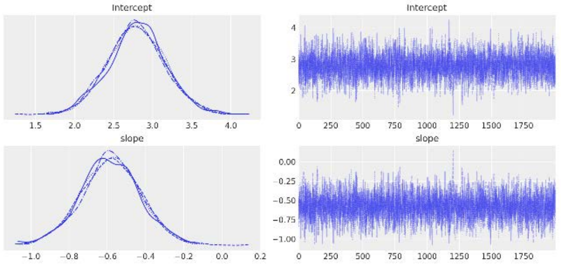

Fig. 7 Bayesian analysis results for all data

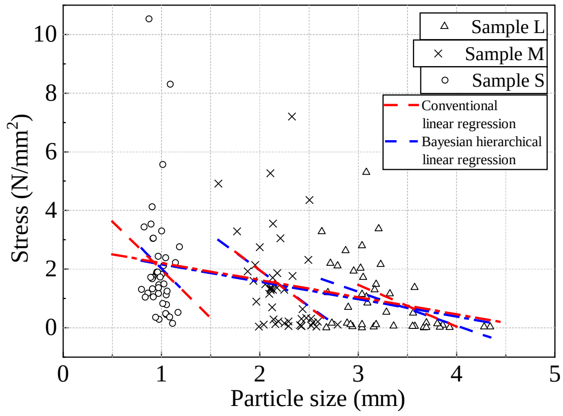

Fig. 8 Data fitting

Table 1 Fitting equation result

Method	Sample	Equation
Frequentist	All Data	y = 2.756 – 0.593x
	Sample L	y = 4.707 - 1.159x
	Sample M	y = 6.828 - 2.434x
	Sample S	y = 5.414 – 3.394x
Bayesian	All Data	y = 2.791 – 0.582x
	Sample L	y = 5.741 – 1.426x
	Sample M	y = 6.982 – 2.511x
	Sample S	y = 5.269 – 3.292x

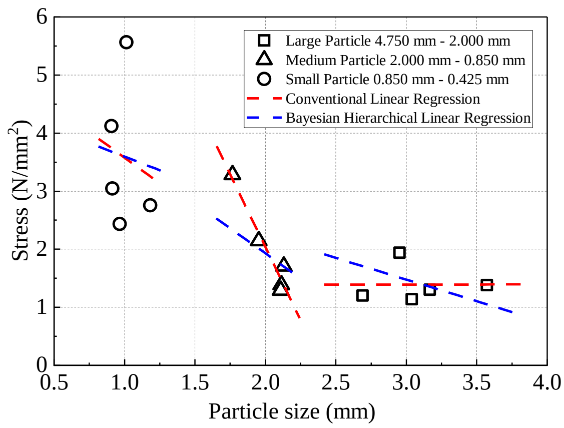

Fig. 9 Crushability test with limited sample [23]

If we compare with previous studies carried out single-particle crushability tests with limited data in Fig. 9, showing significant trendline differences between approaches with conventional frequentist and Bayesian hierarchical models, as shown in Fig. 9. If we compare Fig. 8 and Fig. 9, it is clear that the Bayesian hierarchical model has a significant impact when we use a limited sample, so conventional frequentist and Bayesian hierarchical models will show similar results when we have a sufficient sample.

4.3 Particle Shape

The illustration in Fig. 10 (a) depicts particle shape. Two parameters commonly utilized in analyzing particle shape are aspect ratio and roundness. The image depicts an analysis of the aspect ratio, which is calculated based on Eq. (5).

$$aspect\ ratio = \frac{major\ axis}{minor\ axis} \tag{5}$$

Fig. 10 (b) is an illustration presented for calculating the roundness coefficient, which can be computed using Eq. (6), P is the perimeter of the sample and A is the area of the sample.

$$roundness\ coefficient = \frac{P^2}{4 \times \pi \times A} \tag{6}$$

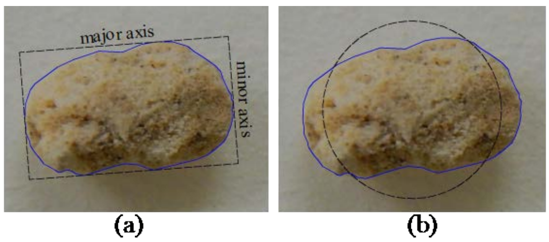

Fig. 10 Analysis of particle shape

4.3.1 Aspect ratio

Based on the aspect ratio calculation, a comparison was made with the results of single-particle crushability strength, as shown in the figure below. In Fig. 11 the analysis results show that the relationship between aspect ratio and single particle strength is scattered and tends not to show a strong relationship between the two parameters. Regarding limitations, the data used in this study does not show a clear relationship, and it is necessary to carry out other measurement variations.

4.3.2 Roundness

The comparison between the roundness calculation and the single-particle crushability test results yielded little correlation between the two parameters shown in Fig. 12, which is similar to the graph presented above in Fig. 12.

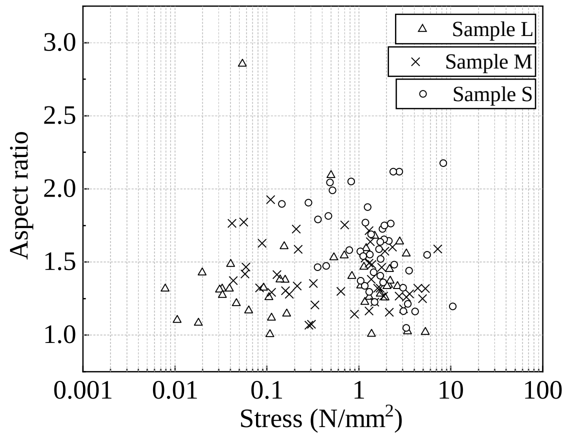

Fig. 11 The relationship between stress and aspect ratio

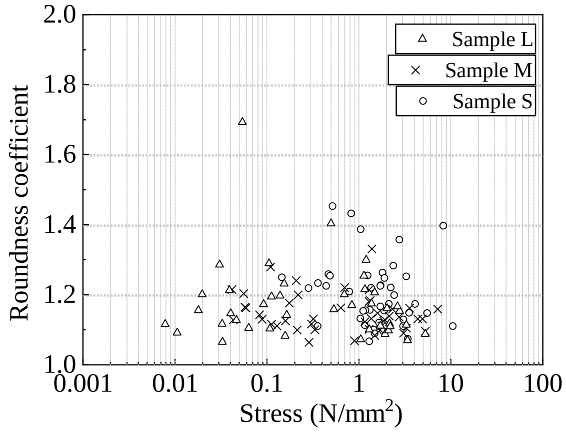

Fig. 12 The relationship between stress and roundness coefficient

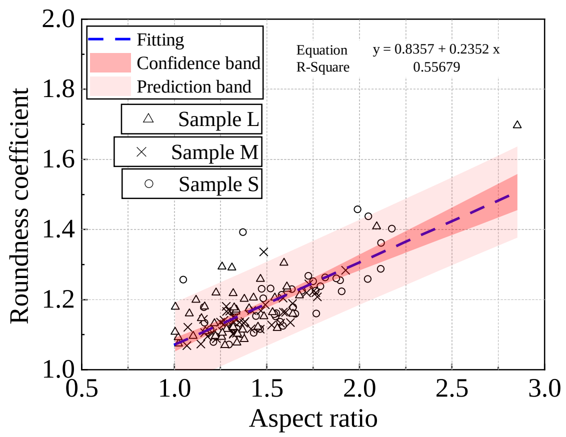

Fig. 13 The relationship between aspect ratio and roundness coefficient

4.3.3 Comparison

Fig. 13 illustrates the comparison between aspect ratio and roundness, and it demonstrates a positive correlation between the roundness coefficient and aspect ratio, whereby an increase in the roundness coefficient value accompanies an increase in the aspect ratio value.

4.4 Microstructural

The microstructural properties of pumice particles were investigated regarding changes in pore characteristics before and after single-particle crushability testing using SEM analysis. As shown in Fig. 14, the initial state of the red colored revealed the presence of pores. Subsequently, Fig. 15 shows the SEM test results after completing single-particle crushability testing on the pumice particles. In the comparison, two different particles were used because the material needs to be coated during SEM and EDS testing, so the material cannot be tested as a single particle after SEM and EDS testing. The results of the changes in pore volume are presented in Table 2. The table indicates a reduction in pore area in pumice particles due to the applied pressure. Conversely, as the area decreases, the number of counted pores increases. This observation suggests that under significant pore loading, the pores undergo constriction, and new tiny pores emerge due to cracks induced by the loading on the pumice.

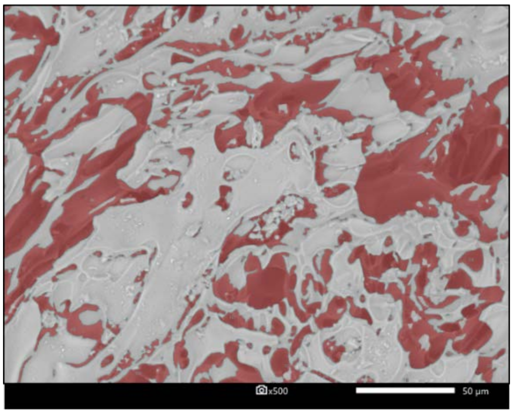

Fig. 14 Pore of pumice sand before crushing

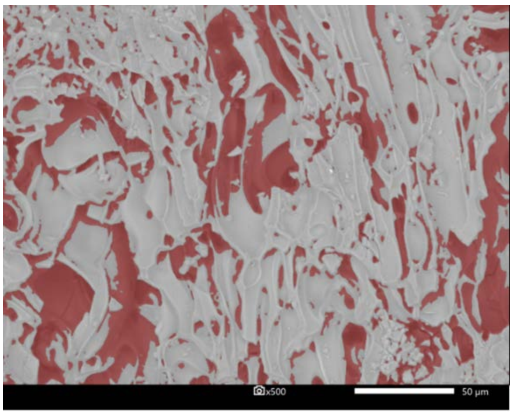

Fig. 15 Pore of pumice sand after crushing

Table 2 Number of pores before and after the test

	Before	After
Count	245	406
Total area pore (μm^2)	18569.16	14535.81
Average size total area pore (μm^2)	75.792	35.802
Area pore (%)	37.395	29.398

5. CONCLUSIONS

In this study, pumice particles were subjected to a single-particle crushability test, followed by the analysis of their chemical and microstructural components using SEM and EDS. The results can be summarized as follows:

1 The chemical composition of Pumice sand from Miyakonojo area is primarily comprised of Oxygen (O), Silica (Si), and Alumina (Al), with other chemical components present in lesser quantities. This substance is analogous to typical pumice, which is primarily comprised of silica (SiO_2) and alumina (Al_2O_3).

2 The relationship between particle size and particle strength exhibits a negative trend, whereby an increase in particle size results in a decrease in particle stress.

3 The frequentist and Bayesian analyses of the linear relationship between particle size and particle stress do not exhibit significant differences due to the large sample size.

4 The relationship between the parameter aspect ratio and roundness coefficient with particle stress does not exhibit a significant correlation.

5 The aspect ratio and roundness coefficient exhibit a positive correlation, whereby an increase in aspect ratio is followed by an increase in roundness coefficient, resembling that of typical crushable soil.

6 There is a reduction in the pore area of pumice particles, while the number of pores present has increased due to the single-particle crushability test.

6. ACKNOWLEDGMENTS

The authors are grateful to the Japanese Government (MEXT) and JICA (Innovative Asia) for supporting the first author during his Ph.D. studies at Kyushu University. We also thank Mr. Yuichi Yahiro and The Ultramicroscopy Research Center Kyushu University for providing technical support.

7. REFERENCES

[1] Fisher R. V., Proposed Classification of Volcaniclastic Sediments and Rocks, Bulletin of the Geological Society of America, Vol. 72, No. 9, 1961, pp. 1409–1414.

[2] McPhie J., Doyle M., and Allen R., Volcanic Texture: a Guide to the Interpretation of Textures in Volcanic Rocks. Tasmania: CODES Key Centre, University of Tasmania, 1993.

[3] Chiaro G., Kiyota T., Umar M., and Cappellaro C., Earthquake-Induced Flow-Type Slope Failure in Weathered Volcanic Deposits—A Case Study: The 16 April 2016 Takanodai Landslide, Japan, Geosciences (Basel), Vol. 12, No. 11, 2022, pp. 1–22.

[4] Hosobuchi M. N., Chigira M., Lim C., and Komoo I., Geological history controlling the debris avalanches of pyroclastic fall deposits induced by the 2009 Padang earthquake, Indonesia: The sequential influences of pumice fall, weathering, and slope undercut, Eng Geol, Vol. 287, 2021, pp. 1–15.

[5] Kasama K., Furukawa Z., and Yasufuku N., Cyclic shear property and seismic runout analysis for pumice fall deposit, Soil Dynamics and Earthquake Engineering, Vol. 143, 2021, pp. 1–11.

[6] Nishimura I., Noguchi T., Ono Y., and Kohno M., Subsarface structures based on microtremor observations in landslide area of Tandikat, West Sumatra, Indonesia, International Journal of GEOMATE, Vol. 22, No. 90, 2022, pp. 57–62.

[7] Siebe C., Salinas S., Arana-Salinas L., Macías J. L., Gardner J., and Bonasia R., The ~ 23,500 y14C BP White Pumice Plinian eruption and associated debris avalanche and Tochimilco lava flow of Popocatépetl volcano, México, Journal of Volcanology and Geothermal Research, Vol. 333–334, 2017, pp. 66–95.

[8] Bengtsson M., Empirical Energy and Size Distribution Model for Predicting Single Particle Breakage in Compression Crushing., Mineral Engineering, Vol. 171, 2021, pp. 1–9.

[9] He Y., Cai G., Gao L., and He H., Effect of Particle Size and Constraint Conditions on Single Particle Strength of Carbonate Sand, Sensors, Vol. 22, No. 3, 2022, pp. 1–17.

[10] Yoshimoto N., Hyodo M., Nakata Y., Orense R. P., Hongo T., and Ohnaka A., Evaluation of shear strength and mechanical properties of granulated coal ash based on single particle strength, Soils and Foundations, Vol. 52, No. 2, 2012, pp. 321–334.

[11] Zhao B., Wang J., Coop M. R., Viggiani G., and Jiang M., An investigation of single sand particle fracture using X-ray microtomography,

Géotechnique, Vol. 65, No. 8, 2015, pp. 625–641.
[12] Tavares L. M., Review and Further Validation of a Practical Single-Particle Breakage Model †, KONA Powder and Particle Journal, Vol. 39, 2022, pp. 62–83.
[13] Zhang X., Baudet B. A., and Yao T., The influence of particle shape and mineralogy on the particle strength, breakage and compressibility, International Journal of Geo-Engineering, Vol. 11, No. 1, 2020.
[14] Liburkin R., Portnikov D., and Kalman H., Comparing Particle Breakage in an Uniaxial Confined Compression Test to Single Particle Crush Test-Model and Experimental Result, Powder Technol, Vol. 2015, No. 284, 2015, pp. 344–354.
[15] Liu C., Liu F., Song J., Ma F., Wang D., and Zhang G., On the measurements of individual particle properties via compression and crushing, Journal of Rock Mechanics and Geotechnical Engineering, Vol. 13, No. 2, 2021, pp. 377–389.
[16] Orense R. P., Pender M. J., Hyodo M., and Nakata Y., From Micro to Macro: An Investigation of the Geomechanical Behavior of Pumice Sand, in Volcanic Rocks and Soils, 1st ed., No. 2, T. Rotanda, M. Cecconi, F. Silvestri, and P. Tommasi, Eds., London: CRC Press, 2016, pp. 45–62.
[17] Sumartini W. O., Hazarika H., Kokusho T., Ishibashi S., Matsumoto D., and Chaudhary B., Deformation and Failure Characteristics of Volcanic Soil at Landslides Site due to the 2016 Kumamoto Earthquake, International Association of Lowland Technology, Vol. 19, No. 4, 2018, pp. 237–244
[18] Kikkawa N., Pender M. J., and Orense R. P., Comparison of the Geotechnical Properties of Pumice Sand from Japan and New Zealand, in Proceedings of the 18th International Conference on Soil Mechanics and Geotechnical Engineering, 2013, pp. 239–242.
[19] Baecher G. B., Bayesian thinking in geotechnics (2nd Lacasse Lecture), in Geo Risk, Denver: American Society of Civil Engineers (ASCE), Jun. 2017, pp. 1–18.
[20] Contreras L. F., Brown E. T., and Ruest M., Bayesian data analysis to quantify the uncertainty of intact rock strength, Journal of Rock Mechanics and Geotechnical Engineering, Vol. 10, No. 1, 2018, pp. 11–31.
[21] Kobayashi M., Kuroda R., Suzuki K., and Fukao Y., Models for the Origin of the Pumice Associated with the 1989 Submarine Eruption Off-Ito, Central Honshu, Japan, J. Phys. Earth, Vol. 39, 1991, pp. 21–26.
[22] Mboya H. A., Makunza J., and Mwishwa Y. H. B., Assessment of Pumice Blocks in Comparison to Cement Sand Blocks and Burnt Blocks "The Case of Mbeya City - Tanzania," Journal of Civil Engineering Research and Practice, Vol. 8, No. 1, 2011, pp. 43–55.
[23] Basoka I. W. A., Kasama K., and Furukawa Z., Linear Regression Model of Pumice Particle Strength, in 58th Japan National Conference on Geotechnical Engineering, Fukuoka, Jul. 2023, pp. 2266–2267.